THE JOURNAL OF PHYSICAL CHEMISTRY A

Article

pubs.acs.org/JPCA

Theoretical ab Initio Study of the Series of N_2X^+ Cations with X = F, Cl, Br, and I. New Insights on the "Unusual" N_2F^+ Species

Aristotle Papakondylis*

Department of Chemistry, Laboratory of Physical Chemistry, National and Kapodistrian University of Athens, Panepistimiopolis Zografou, Athens 157 71, Greece

ABSTRACT: The series of cations $N_2X^+(\tilde{X}^1\Sigma^+)$, with X = F, Cl, Br, I, has been theoretically studied by variational multireference CI and coupled-cluster techniques in conjunction with basis sets of quintuple-ζ quality. We report electronic and geometric structure data and harmonic frequencies as well as binding energies and potential energy curves. A new rationalization is provided for the bonding mode in N_2F^+, which provides an explanation for the unusually short N−F bond.

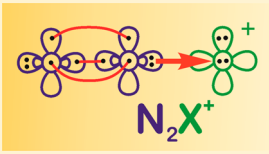

1. INTRODUCTION

The fluorodiazonium cation, N_2F^+, became famous as an important precursor in the synthesis of N_5^+ by Christe et al.[1] It was first prepared by Moy and Young II[2] some 50 years ago. These researchers used the reaction of *cis*-difluorodiazine with arsenic pentafluoride to produce a white solid identified as the $N_2F^+AsF_6^-$ ionic compound. The presence of N_2F^+ in this solid was further confirmed a few years later by Shamir and Bineboym[3] and Christe et al.[4] through Raman and infrared spectroscopy. These workers concluded that N_2F^+ is linear and asymmetric and that the N−N bond has a triple bond character. The first ab initio study on N_2F^+ was reported in 1975 by Pulay et al.[5] who performed Hartree−Fock calculations to predict the r_{N-F} = 1.28 Å and r_{N-N} = 1.10 Å bond distances and also the vibrational force constants. In 1978, Peters[6] employed the MP2/6-31G* method to find r_{N-F} = 1.256 Å, r_{N-N} = 1.138 Å and a heat of formation ΔH_f^0 = 329 kcal/mol. The first crystallographic study of $N_2F^+AsF_6^-$ salt was carried out in 1991 by Christe et al.[7] They found a total $r_{N-F} + r_{N-N}$ = 2.316 Å distance which was empirically partitioned as r_{N-F} = 1.217 Å and r_{N-N} = 1.099 Å. In the same work theoretical calculations at the LDF level gave r_{N-F} = 1.225 Å and r_{N-N} = 1.106 Å and vibrational frequencies in good agreement with experiment. It was pointed out by these authors that the N−F bond length in N_2F^+ is the shortest observed between the two elements. As an explanation to this fact the sp-hybridization of the terminal N atom was invoked. A subsequent millimeter-wave spectroscopic investigation of the gas-phase structure of N_2F^+ by Botschwina et al.[8] yielded r_{N-F} = 1.2461 Å and r_{N-N} = 1.1034 Å. These authors also performed CEPA calculations with relatively small basis sets to find r_{N-F} = 1.2612 Å, somewhat larger than their experimental number. From these values it is clear that the N−F bond length is much smaller than its typical value of ∼1.35 Å but also that the N_2 moiety preserves its triply bonded N−N distance. In 1995 Cacace et al.[9] reported production of gaseous N_2F^+ from the ionization of NF_3/HN_3 mixtures. The mechanism of formation of fluorodiazonium ions was investigated by MIKE and FT-ICR spectrometries combined with post-SCF ab initio calculations. The problem of the short N−F bond in N_2F^+ was revisited in 2002 by Bickelhaupt et al.[10] These authors performed density functional calculations at the BP86/TZ2P level to obtain r_{N-F} = 1.245 Å and r_{N-N} = 1.112 Å as well as a binding energy D_e = 102.5 kcal/mol with respect to the $N_2^+(X^2\Sigma_g^+)$ + $F(^2P)$ dissociation channel. They also claimed that reduced steric and Pauli repulsion effects are responsible for the short N−F bond, a conclusion that was at variance with the Christe at al.[7] assumption about sp-hybridization of the N atom. A different rationalization was presented by Harcourt[11] on the basis of valence bond (VB)/STO-3G calculations. He proposed that the dominant Lewis-type VB structures are those involving a single positive charge on either of the N atoms. Moreover he suggested that N−F π-bonding is one of the factors responsible for the shortening of the N−F bond of N_2F^+ relative to that of NF_4^+. In a recent paper Christe at al.[12] were able for the first time to obtain the individual N−N and N−F distances in the solid state; through crystallographic analysis of the newly prepared $N_2F^+Sb_2F_{11}^-$ solid they found r_{N-F} = 1.257 Å and r_{N-N} = 1.089 Å which are among the shortest experimentally observed N−F and N−N bonds. They also used the CCSD(T)/aug-cc-pVTZ methodology to calculate r_{N-F} = 1.2357 Å and a heat of formation ΔH_f(0 K) = 291.2 kcal/mol.

From the foregoing discussion it becomes quite clear that one has to deal with a rather "unusual" cation. N_2F^+ has a ground state of $\tilde{X}^1\Sigma^+$ symmetry. Its potential energy surface correlates adiabatically to the ground state fragments $N_2^+(X^2\Sigma_g^+)$ + $F(^2P)$ since the ionization potentials IP(N_2) < IP(F). However, as we will see later the particular electronic structure of $N_2^+(X^2\Sigma_g^+)$ (vide infra) cannot favor a strong covalent N−F bond as is thought so far. In the present study we attempt to show that the intrinsic electronic configuration of N_2F^+ corresponds to a higher asymptotic channel, namely $N_2(X^1\Sigma_g^+)$ + $F^+(^1D)$, explaining the peculiar character of the cation. Although lying higher than the $N_2^+(X^2\Sigma_g^+)$ + $F(^2P)$ asymptote, by ∼4.4 eV, it will be shown that it can be significantly stabilized when involved in the bonding.

Received: October 17, 2016
Revised: November 14, 2016
Published: November 14, 2016

DOI: 10.1021/acs.jpca.6b10471
J. Phys. Chem. A 2016, 120, 9660−9666

To complete this study we also considered the homologous N_2X^+ cations with X = Cl, Br, and I. Curiously enough we did not find any experimental or theoretical data on these cations. As it will be shown below they all have bound $\tilde{X}^1\Sigma^+$ ground states similar to those for N_2F^+. However, the corresponding adiabatic dissociation channel is now $N_2(X^1\Sigma_g^+) + X^+(^1D)$.

In what follows we present a thorough comparative theoretical investigation of the four N_2X^+ (X = F, Cl, Br, I) cationic systems. We have employed high level ab initio multireference CI and coupled-cluster methods combined with large basis sets to determine structural and spectroscopic constants as well as binding energies and potential energy curves (PEC). Useful accurate data for the yet unknown N_2Cl^+, N_2Br^+, and N_2I^+ cations are provided for the first time.

2. COMPUTATIONAL DETAILS

Our computational approach comprises multireference configuration interaction (MRCI) as well as coupled-cluster (CC) methods.

For all calculations we employed the quintuple-ζ correlation consistent cc-pV5Z basis sets for N, F,[13] Cl,[14] and Br[15] and cc-pV5Z-PP for the I[16] atom. The cc-PV5Z-PP basis uses a relativistic core potential to replace 28 electrons ($[Ar]3d^{10}$) of iodine.

In the coupled cluster calculations, we used the single reference (restricted Hartree−Fock) partially spin restricted open-shell coupled-cluster singles and doubles with a perturbative treatment of triples RCCSD(T)[17−19] formalism.

For the multireference calculations, we followed the complete active space self-consistent field (CASSCF) + single + double replacements method (CASSCF + 1 + 2 = MRCI). The reference space was defined by allotting all eight σ valence electrons of each cation to eight orbitals of same symmetry. This yields a total of 1764 reference configuration functions (CF). The remaining 8 valence electrons of π symmetry were included in the singles and doubles (CISD) correlation treatment. The final MRCI space consists of $\sim 10^7$ CF's and was internally contracted[20] to $\sim 5.5 \times 10^6$ CF's. To take into account the size nonextensivity error (SNE) of $\sim 30mE_h$ at the MRCI level the Davidson correction[21] for unlinked quadruples was applied (MRCI+Q) which reduced the SNE to $\sim 14mE_h$.

In all cases, the basis set superposition error (BSSE) never exceeded 0.5 kcal/mol, which is beyond chemical interest.

Harmonic frequencies were calculated by diagonalizing the Hessian matrix at the RCCSD(T)/cc-pV5Z level.

All calculations were performed with the MOLPRO2012.1 program.[22,23]

3. RESULTS AND DISCUSSION

A. General Insights and the N_2H^+ Cation. Considering the ground $\tilde{X}^1\Sigma^+$ states of the N_2X^+ cations, where X = F, Cl, Br, and I, we will explore the possible lowest asymptotic channels correlating adiabatically to these species. Depending on the ionization potentials (IP) of the two entities, N_2 and X, we have the following possibilities:

(a) if $IP(N_2) < IP(X)$, then obviously

$$N_2^+(X^2\Sigma_g^+) + X(^2P) \rightarrow N_2X^+(\tilde{X}^1\Sigma^+) \quad (1)$$

but,

(b) if $IP(N_2) > IP(X)$, the situation is not that clear because the ground state fragments $N_2(X^1\Sigma_g^+) + X^+(^3P)$ cannot yield a singlet $N_2X^+(\tilde{X}^1\Sigma^+)$ state. The lowest compatible asymptote is now $N_2(X^1\Sigma_g^+) + X^+(^1D)$ where X^+ finds itself in its first ^1D excited state. In this case, we have

$$N_2(X^1\Sigma_g^+) + X^+(^1D) \rightarrow N_2X^+(\tilde{X}^1\Sigma^+) \quad (2)$$

Now, of course, to decide upon the lowest asymptote we need to take into account, as well, the $X^+(^1D) \leftarrow X^+(^3P)$ excitation energy, i.e., to compare $IP(N_2)$ with $IP(X) + \Delta E[X^+(^1D) \leftarrow X^+(^3P)] \equiv \Delta E[X^+(^1D) \leftarrow X(^2P)]$. If $IP(N_2) > \Delta E[X^+(^1D) \leftarrow X(^2P)]$ then eq 2 represents the lowest adiabatic process. In the opposite case, the same holds for eq 1.

Table 1 summarizes our results along with the corresponding experimental values on the above quantities of interest. First we note the very good agreement of our calculated numbers with experiment. Second, it is clear that the N_2F^+ cation must follow eq 1 and adiabatically correlate to the $N_2^+(X^2\Sigma_g^+) + F(^2P)$

Table 1. Results and Experimental Values

(a) Ionization Potentials IP(X) (eV) of X, Separation Energies $\Delta E[X^+(^1D) \leftarrow X^+(^3P)]$ (eV) of X^+, and $\Delta E[X^+(^1D) \leftarrow X(^2P)] = IP(X) + \Delta E[X^+(^1D) \leftarrow X^+(^3P)]$, for X = F, Cl, Br, and I

method	IP(X)	$\Delta E[X^+(^1D) \leftarrow X^+(^3P)]$	$\Delta E[X^+(^1D) \leftarrow X(^2P)]$
		F	
MRCI	17.22	2.68	19.90
MRCI+Q	17.32	2.58	19.90
RCCSD(T)	17.36	2.76	20.12
expt[a]	17.43	2.57	20.00
		Cl	
MRCI	12.77	1.43	14.20
MRCI+Q	12.88	1.48	14.36
RCCSD(T)	12.92	1.58	14.50
expt[a]	12.97	1.40	14.37
		Br	
MRCI	11.67	1.31	12.98
MRCI+Q	11.78	1.31	13.09
RCCSD(T)	11.80	1.39	13.19
expt[a]	11.84	1.32	13.16
		I	
MRCI	10.38	1.07	11.45
MRCI+Q	10.49	1.01	11.50
RCCSD(T)	10.51	1.17	11.68
expt[a]	10.52	1.32	11.84

(b) Energies E (E_h), Bond Lengths r_e (Å) of $N_2(X^1\Sigma_g^+)$ and $N_2^+(X^2\Sigma_g^+, B^2\Sigma_u^+)$, and Ionization Potential $IP(N_2)$ (eV) of $N_2(X^1\Sigma_g^+)$.

method	$-E$	r_e	$IP(N_2)$
	$N_2(X^1\Sigma_g^+)$		
MRCI	109.374 25	1.0884	15.72
MRCI+Q	109.407 86	1.0979	15.53
RCCSD(T)	109.414 20	1.0995	15.58
expt[b]		1.097 68	15.58
	$N_2^+(X^2\Sigma_g^+)$		
MRCI	108.796 39	1.1036	
MRCI+Q	108.837 09	1.1158	
RCCSD(T)	108.841 44	1.1177	
expt[b]		1.1164	
	$N_2^+(B^2\Sigma_u^+)$		
MRCI	108.674 20	1.0542	
MRCI+Q	108.723 73	1.0744	
RCCSD(T)	–	–	
expt[b]		1.0742	

[a]Reference 24; all values are M_J-averaged. [b]Reference 25.

DOI: 10.1021/acs.jpca.6b10471
J. Phys. Chem. A 2016, 120, 9660−9666

fragments. For all other N_2X^+ (X = Cl, Br, I) the situation is reversed since $IP(N_2) > \Delta E[X^+(^1D) \leftarrow X(^2P)]$ and eq 2 now reflects the lowest adiabatic process.

Next we will try to get some insights on the nature of the interactions as described by eqs 1 and 2. To this end we considered the simpler N_2H^+ diazenylium system. This cation was one of the first ions to be observed in interstellar clouds and has been previously studied.[26] Figure 1 shows potential

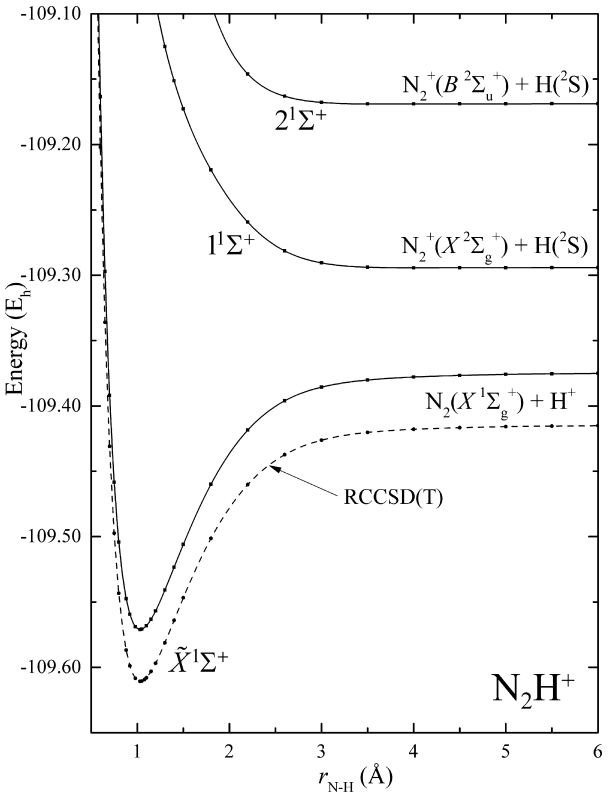

Figure 1. Potential energy curves for the collinear approaches $N_2(X^1\Sigma_g^+)$ + H^+ and $N_2^+(X^2\Sigma_g^+, B^2\Sigma_u^+)$ + $H(^2S)$ at the MRCI/cc-pV5Z level of theory.

energy curves (PEC) for the linear approaches N_2 + H^+ and N_2^+ + H. Of course the ground $N_2H^+(\tilde{X}^1\Sigma^+)$ state correlates adiabatically to $N_2(X^1\Sigma_g^+)$ + H^+ since $IP(N_2) > IP(H)$. All our results concerning N_2H^+ are reported on Table 2. As we can see an important $N_2 \rightarrow H^+$ charge transfer of ~0.8 e^- is followed by a rather large N−H binding energy D_0 = 116.5 kcal/mol. Consequently and according to our findings the bonding can be depicted by the valence bond−Lewis (vbL) diagram of Scheme 1. As shown in this diagram, a dative $N \rightarrow H^+$ bond is formed.

This bond is reinforced by the strong Coulombic attraction exercised by the proton on the $2s^2$ electron pair of the terminal nitrogen atom. As no electron recoupling is needed we were

Scheme 1. Interaction of $N_2(X^1\Sigma_g^+)$ with H^+

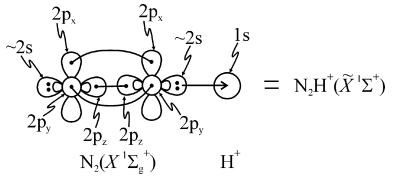

able to construct a ground state PEC also with the single reference RCCSD(T) method, Figure 1.

We turn now to the next asymptotic channel $N_2^+(X^2\Sigma_g^+)$ + $H(^2S)$. From Figure 1, we can see that this interaction results in a repulsive PEC. In order to explain this fact we have to take a careful look at the electronic structure of $N_2^+(X^2\Sigma_g^+)$. The corresponding electronic distribution according to our calculations is $1\sigma_g^2 1\sigma_u^2 2\sigma_g^2 2\sigma_u^2 1\pi^4 3\sigma_g^1$. Now inspecting the singly occupied $3\sigma_g$ orbital we found that it mostly corresponds to the σ-bond of N_2. Thus, the interaction with H can be described by the vbL diagram of Scheme 2. From this diagram, it is clear that electron coupling to form a covalent N_2^+−H bond can hardly take place.

Scheme 2. Interaction of $N_2^+(X^2\Sigma_g^+)$ with $H(^2S)$

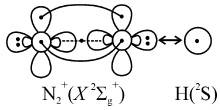

Indeed, according to our calculations the leading CI configuration all along the $N_2^+(X^2\Sigma_g^+)$ + $H(^2S)$ curve corresponds to an open singlet as shown in Scheme 2. This last finding will play an important role in the upcoming discussion on the nature of bonding in N_2F^+.

B. N_2F^+. All our numerical results concerning the $\tilde{X}^1\Sigma^+$ ground state of N_2F^+ are reported on Table 3. As we can see our calculated bond lengths and harmonic frequencies are in very good agreement with the corresponding experimental numbers. For the binding energy D_0 with respect to $N_2^+(X^2\Sigma_g^+)$ + $F(^2P)$ there is no experimental number but our results D_0 = 88.9 (MRCI+Q) and 87.4 (RCCSD(T)) kcal/mol lead to ΔH_f^0 = 288 and 291 kcal/mol, respectively, in excellent agreement with the theoretical number 291.2 kcal/mol by Christe et al.[12]

Figure 2 shows three adiabatic PEC's corresponding to the collinear approaches of the $N_2^+(X^2\Sigma_g^+)$ + $F(^2P)$, $N_2^+(B^2\Sigma_u^+)$ + $F(^2P)$, and $N_2(X^1\Sigma_g^+)$ + $F^+(^1D)$ fragments, in ascending energy order $\tilde{X}^1\Sigma^+$, $1^1\Sigma^+$, and $2^1\Sigma^+$, respectively. As a first observation, it is interesting that all three curves possess minima. Next, we are going to attempt a comparison with the PEC's of Figure 1 concerning N_2H^+. The ground state $N_2F^+(\tilde{X}^1\Sigma^+)$ curve correlates adiabatically to the $N_2^+(X^2\Sigma_g^+)$ + $F(^2P)$ asymptote depicted by Scheme 3 which is analogous to $N_2^+(X^2\Sigma_g^+)$ +

Table 2. Energies E (E_h), Bond Distances r (Å), Binding Energy D_0 (kcal/mol), Net Mulliken Charge on H q_H (e), and Harmonic Frequencies ω_e (cm^{-1}) of the Ground $\tilde{X}^1\Sigma^+$ State of the N_2H^+ Species

method	−E	r(N−H)	r(N−N)	D_0[a]	q_H	ω_e
MRCI	109.571 06	1.032	1.082	116.2	+0.18	–
MRCI+Q	109.604 21	1.034	1.085	116.2		–
RCCSD(T)	109.610 67	1.034	1.095	116.5		(π) 698, (σ^+) 2297, (σ^+) 3407
expt.		1.0346[b]	1.0927[b]			(π) 687,[c] (σ^+) 2258,[c] (σ^+) 3234[c]

[a]With repect to $N_2(X^1\Sigma_g^+)$ + H^+. [b]Reference 27. [c]Reference 28.

DOI: 10.1021/acs.jpca.6b10471
J. Phys. Chem. A 2016, 120, 9660−9666

Table 3. Energies E (E_h), Bond Distances r (Å), Binding Energies D_e and D_0 (kcal/mol), Net Mulliken Charges on the Halogen Atom X q_X (e),[a] and Harmonic Frequencies ω_e (cm^{-1}) of the Ground $\tilde{X}^1\Sigma^+$ States of the N_2X^+ Species, with X = F, Cl, Br, and I

method	$-E$	r(N–X)	r(N–N)	D_e[b]	D_0[b]	q_X	ω_e
				N_2F^+			
MRCI	208.562061	1.243	1.084	94.8	92.0	+0.18	–
MRCI+Q	208.627 49	1.246	1.084	91.6	88.9		–
RCCSD(T)	208.645814	1.247	1.105	90.3	87.4		(π) 406, (σ^+) 1058, (σ^+) 2391
expt.		1.2461[c]	1.1034[c]				(π) 385, (σ^+) 1057, (σ^+) 2389[d]
		1.257[d]	1.089[d]				
				N_2Cl^+			
MRCI	568.636520	1.609	1.087	94.8	92.8	+0.38	–
MRCI+Q	568.708 67	1.611	1.087	96.9	94.9		–
RCCSD(T)	568.728839	1.602	1.107	92.8	90.8		(π) 383, (σ^+) 693, (σ^+) 2288
				N_2Br^+			
MRCI	2681.575934	1.801	1.086	68.1	66.5	+0.51	–
MRCI+Q	2681.642 72	1.805	1.086	70.3	68.7		–
RCCSD(T)	2681.661645	1.791	1.105	65.8	64.3		(π) 339, (σ^+) 505, (σ^+) 2291
				N_2I^+			
MRCI	403.789746	2.055	1.086	44.8	43.5	+0.70	–
MRCI+Q	403.853 02	2.051	1.086	46.4	45.2		–
RCCSD(T)	403.872138	2.041	1.104	42.3	41.0		(π) 295, (σ^+) 381, (σ^+) 2303

[a]Net Mulliken charges using the MRCI density. [b]With respect to $N_2^+(X^2\Sigma_g^+)$ + $F(^2P)$ for N_2F^+, or $N_2(X^1\Sigma_g^+)$ + $X^+(^1D)$ for N_2X^+, with X = Cl, Br, I. [c]Gas phase.[8] [d]Solid state.[12]

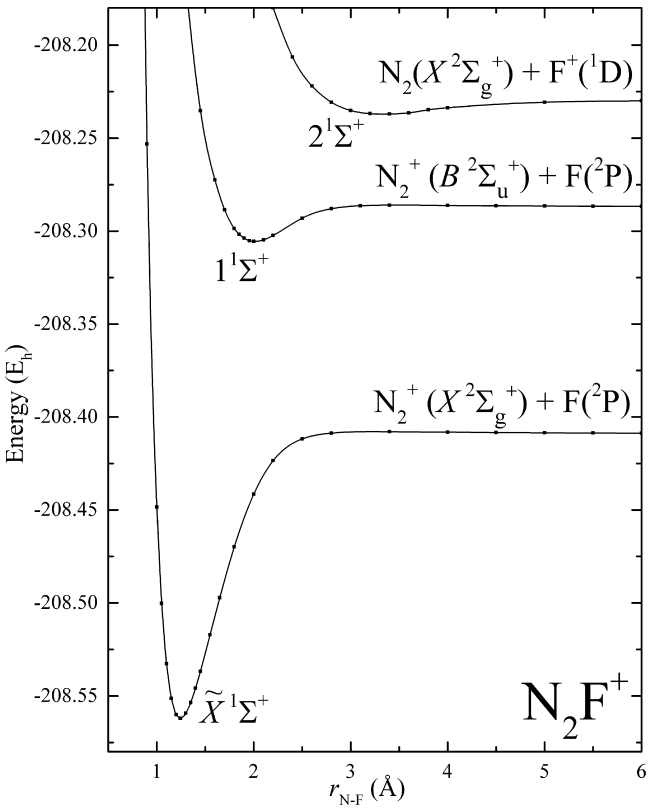

Figure 2. Potential energy curves for the collinear approaches $N_2^+(X^2\Sigma_g^+, B^2\Sigma_u^+)$ + $F(^2P)$ and $N_2(X^1\Sigma_g^+)$ + F^+ at the MRCI/cc-pV5Z level of theory.

Scheme 3. Interaction of $N_2^+(X^2\Sigma_g^+)$ with $F(^2P)$

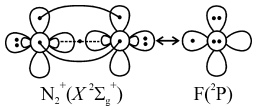

$H(^2S)$ shown in Scheme 2. The latter gives rise to the $N_2H^+(1^1\Sigma^+)$ PEC which is completely repulsive, Figure 1. As previously seen the N_2H^+ ground state is formed from $N_2(X^1\Sigma_g^+)$ + H^+. This is similar to the $N_2(X^1\Sigma_g^+)$ + $F^+(^1D)$ interaction outlined in Scheme 4. In this scheme only the first term of the $|^1D, M_L = 0\rangle = \frac{1}{\sqrt{6}}(2|p_x^2 p_y^2| - |p_x^2 p_z^2| - |p_y^2 p_z^2|)$ wave function of F^+ is shown.

Scheme 4. Interaction of $N_2(X^1\Sigma_g^+)$ with $F^+(^1D)$

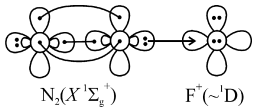

The charge transfer mechanism indicated here is completely analogous to the one of Scheme 1. However, the resulting curve $2^1\Sigma^+$ of N_2F^+, Figure 2, only has a shallow minimum of ~8.6 kcal/mol at a large, r_{N-F} = 3.17 Å, distance as computed at the MRCI+Q level. Finally, from Figure 2, we see that the $N_2F^+(1^1\Sigma^+)$ curve has a minimum at r_{N-F} = 1.96 Å with D_e = 16 kcal/mol. This curve correlates to $N_2^+(B^2\Sigma_u^+)$ + $F(^2P)$ in analogy with the $N_2H^+(2^1\Sigma^+)$ curve correlating to $N_2^+(B^2\Sigma_u^+)$ + $H(^2S)$. The latter is totally repulsive. Now, in order to rationalize all these differences with N_2H^+ and also with the rest of N_2X^+ cations (vide infra) we have monitored the contribution of the two configurations described by Schemes 3 and 4 in the total $N_2F^+(\tilde{X}^1\Sigma^+)$ MRCI wave function all along the ground state PEC. Figure 3 displays the evolution of the squared MRCI coefficients corresponding to the two configurations. As we can see, the initially dominant $N_2^+(X^2\Sigma_g^+)$ + $F(^2P)$ coefficient (C_1) reaches equilibrium with an approximately zero value. On the other hand, the $N_2(X^1\Sigma_g^+)$ + $F^+(^1D)$ coefficient (C_2) gradually rises from zero to finally dominate the equilibrium wave function. This is a strong evidence for the involvement of the N_2 + $F^+(^1D)$ asymptote to the formation of the N_2F^+ ground state. In other words the in situ electronic structure of N_2F^+ should rather be described by

DOI: 10.1021/acs.jpca.6b10471
J. Phys. Chem. A 2016, 120, 9660–9666

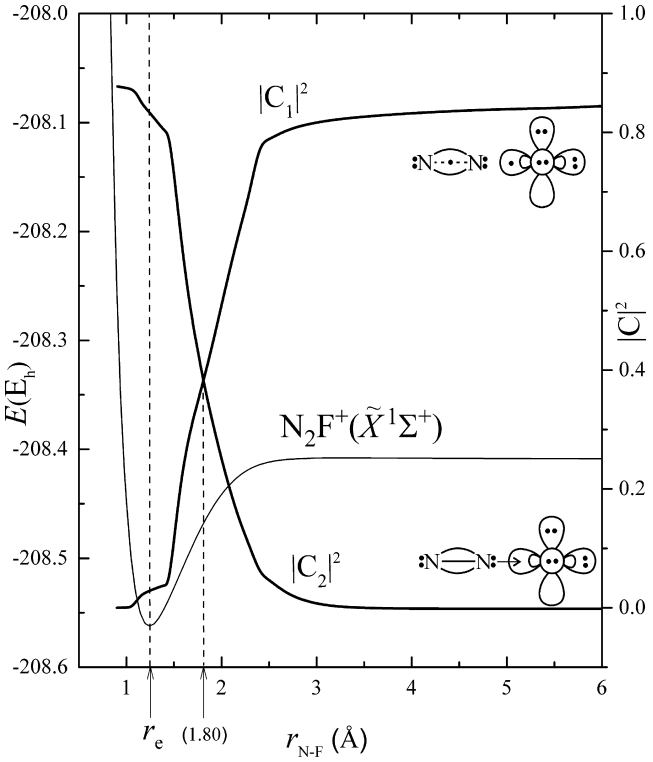

Figure 3. Squared MRCI coefficients (bold lines) of the configurations described by Schemes 3 (C_1) and 4 (C_2) along the adiabatic ground state PEC of $N_2F^+(\tilde{X}^1\Sigma^+)$ at the MRCI/cc-pV5Z level of theory.

Scheme 4. The ensuing avoided crossings should then be responsible for the minima observed on the $1^1\Sigma^+$ and $2^1\Sigma^+$ PEC's. Please notice that this would be the situation with N_2H^+ if the $N_2(X^1\Sigma_g^+)$ + H^+ asymptote was located above $N_2^+(B^2\Sigma_u^+)$ + $H(^2S)$, Figure 1. Now, if this scenario is true, the N_2F^+ cation has an intrinsic, i.e. with respect to $N_2(X^1\Sigma_g^+)$ + $F^+(^1D)$, binding energy D_e as large as $D_e(N_2{-}F^+)+\Delta E[X^+(^1D) \leftarrow X(^2P)]-IP(N_2)$ = ∼ 195 kcal/mol justifying the unusually short N−F bond. We will show in the next section that this value could be expected on the basis of our findings on the rest of N_2X^+ cations, with X = Cl, Br, I. We also mention at this point that, in a theoretical paper[31] of 1992, Christe and Dixon used the LDF method to predict a F^+ detachment energy of 139.3 kcal/mol for N_2F^+. If we add to this the $F^+(^1D) \leftarrow F^+(^3P)$ excitation energy of 59.3 kcal/mol we get 198.6 kcal/mol.

C. N_2X^+ with X = Cl, Br, I. For the homologous to N_2F^+ cations N_2Cl^+, N_2Br^+, and N_2I^+ we have constructed adiabatic PEC's corresponding again to the collinear approaches of $N_2(X^1\Sigma_g^+)$ + $X^+(^1D)$, $N_2^+(X^2\Sigma_g^+)$ + $X(^2P)$, and $N_2^+(B^2\Sigma_u^+)$ + $X(^2P)$. Figure 4 displays curves obtained at the MRCI/cc-pV5Z level for all three cations. Ground state PEC's at the RCCSD(T)/cc-pV5Z level of theory are also given. As we can see the three graphs of Figure 4 are very similar and they also closely resemble the graph of Figure 1 concerning N_2H^+. In all cases we have bound ground states with linear geometry formed from the lowest $N_2(X^1\Sigma_g^+)$ + $X^+(^1D)$ asymptotic products. The bonding can be illustrated by Scheme 4; i.e., the 2s electron pair of the terminal N atom penetrates the empty p orbital of $X^+(^1D)$, forming a harpoon-like dative bond. From Table 3, we see that 0.6, 0.5, and 0.3 e^- are transferred from N_2 to $Cl^+(^1D)$, $Br^+(^1D)$, and $I^+(^1D)$, respectively. Analogously, the D_e values decrease monotonically going down from Cl to Br to I. Corresponding D_0 values are obtained using harmonic frequencies computed at the RCCSD(T)/cc-pV5Z level of theory, Table 3. These values are with respect to the excited $X^+(^1D)$ fragments. In order to calculate D_0^0 numbers we have to subtract the $X^+(^1D) \leftarrow X^+(^3P)$ excitation energies, Table 1, thus getting D_0^0 = 60.8 (N_2Cl^+), 38.5 (N_2Br^+), and 19.6 (N_2I^+) kcal/mol. Taking into account the (experimental[24]) spin−orbit splitting of the $X^+(^3P)$ species the D_0^0 values are further reduced to 59.8 (N_2Cl^+), 34.3 (N_2Br^+), and 10.8 (N_2I^+) kcal/mol with respect to $N_2(X^1\Sigma_g^+)$ + $X^+(^3P_2)$, at the MRCI+Q/cc-

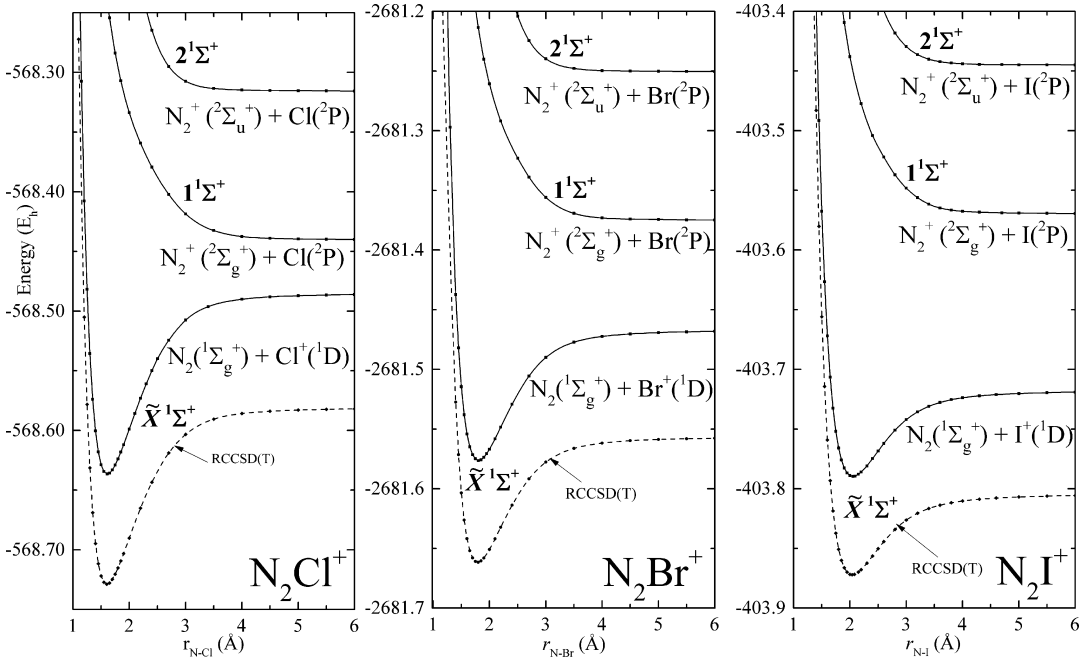

Figure 4. Potential energy curves for the collinear approaches $N_2(X^1\Sigma_g^+)$ + X^+ and $N_2^+(X^2\Sigma_g^+, B^2\Sigma_u^+)$ + $X(^2P)$, with X = Cl, Br, and I, at the MRCI/cc-pV5Z level of theory.

DOI: 10.1021/acs.jpca.6b10471
J. Phys. Chem. A 2016, 120, 9660−9666

pV5Z level. From these numbers we see that all three cations are thermodynamically stable with respect to the ground state N_2 + X^+ products although $D_0^0(N_2I^+)$ is rather low. Probably they could be observed under proper conditions if combined with suitable counter-anions. Unfortunately as mentioned before no experimental or theoretical data exist on any of them.

From Table 3 we see that the N−N bond length is practically unaffected with respect to the free N_2 molecule. For the N−X bonds we found the following equilibrium lengths: 1.61 (N_2−Cl^+), 1.80 (N_2−Br^+), and 2.05 Å (N_2−I^+), Table 3. Comparing the N−Cl bond distance with the corresponding 1.75 Å value encountered in NCl_3,[29] we see that one has to deal with a much shorter than a typical covalent N−Cl bond just like in the case of N_2F^+. On the other hand, ab initio calculations on bromoamines[30] yielded N−Br bond distances ranging between 1.92 and 1.97 Å much greater than r_{N-Br} = 1.80 Å found in N_2Br^+. It seems that the type of bonding described by Scheme 4 allows for a deeper penetration of the nitrogen electron pair into the X^+ electronic cloud, leading to a shorter N−X distance.

Concluding this section we would like to draw attention to an interesting feature of the binding energies D_e of the three N_2X^+ cations. Figure 5 displays a plot of these D_e's vs

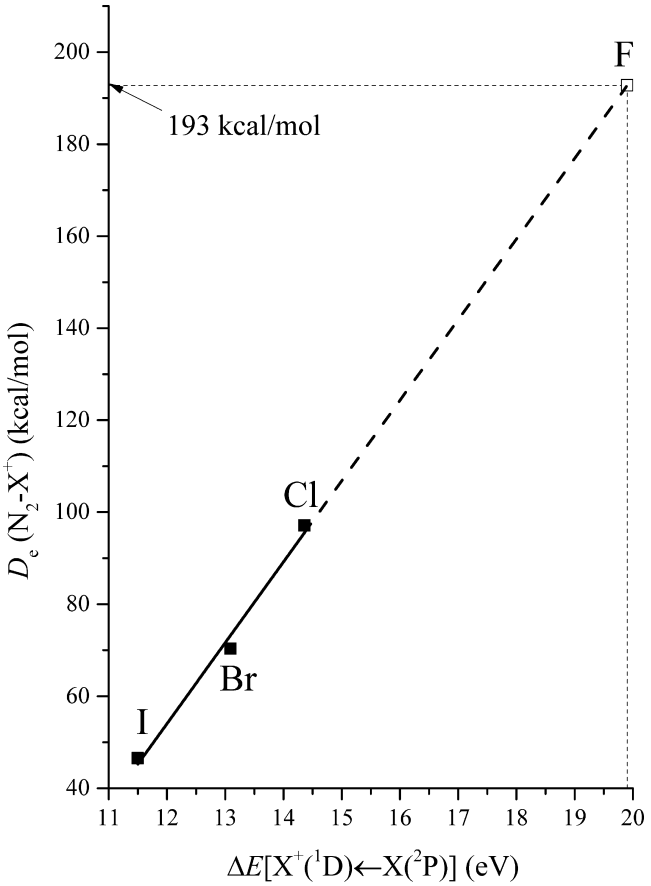

Figure 5. Binding energy $D_e(N_2-X^+)$ as a function of $\Delta E[X^+(^1D) \leftarrow X(^2P)]$ for X = Cl, Br, I, at the MRCI+Q/cc-pV5Z level of theory.

$\Delta E[X^+(^1D) \leftarrow X(^2P)]$ using the MRCI+Q/cc-pV5Z numbers. As we can see there is an excellent linear dependence of D_e on ΔE. The three points fit nicely a straight line which extrapolated for $\Delta E[F^+(^1D) \leftarrow F(^2P)]$ = 19.90 eV (Table 1) gives D_e = ∼ 193 kcal/mol, Figure 5. This number is an estimate of the energy needed for N_2F^+ to (diabatically) reach the $N_2(X^1\Sigma_g^+)$ + $F^+(^1D)$ dissociation channel. Now, if our assumption about the implication of this channel to the formation of N_2F^+ is valid, this number should equal the intrinsic binding energy given by $D_e(N_2-F^+)+\Delta E[X^+(^1D) \leftarrow X(^2P)]-I.P.(N_2)$ as stated in the foregoing discussion on N_2F^+. Using our MRCI+Q results (Tables 1 and 3) we get 91.6 + 458.9−358.1 = 192.4 kcal/mol. Interestingly enough this value is almost identical to the extrapolated 193 kcal/mol number. We believe that this is not an accidental coincidence but rather an additional evidence that the in situ electronic structure of N_2F^+ is described by Scheme 4; a significant charge transfer of ∼0.8 e^- from N_2 to $F^+(^1D)$ stabilizes the system by 193 kcal/mol and places it some 92 kcal/mol below the ground state asymptotic products.

4. SUMMARY AND CONCLUSIONS

We employed multireference CI and RCCSD(T) methods combined with basis sets of quintuple-ζ quality to theoretically study the N_2X^+ cations, with X = F, Cl, Br, and I. They all have linear structures with $\tilde{X}^1\Sigma^+$ ground states and are thermodynamically stable with the following D_0^0 values: 89 (N_2F^+), 60 (N_2Cl^+), 34 (N_2Br^+), and 11 (N_2I^+) kcal/mol with respect to $N_2^+(X^2\Sigma_g^+)$ + $F(^2P)$ or $N_2(X^1\Sigma_g^+)$ + $X^+(^3P_2)$ for X = Cl, Br, I, respectively.

Our numerical results on N_2F^+ are in excellent agreement with existing experimental data. As for N_2Cl^+, N_2Br^+, and N_2I^+, this is the first time, to our knowledge, that they are reported in the literature. We propose here that they could be observed under proper conditions.

We provided evidence that the in situ electronic structure of N_2F^+ corresponds to the excited $N_2(X^1\Sigma_g^+)$ + $F^+(^1D)$ asymptotic channel resulting in a very strong $N_2 \rightarrow F^+(^1D)$ dative bond which stabilizes the system below the ground state asymptotic fragments $N_2^+(X^2\Sigma_g^+)$ + $F(^2P)$, while N_2 preserves its triply bonded character. This type of bonding which naturally occurs in the remaining three cations allows for a closer approach of N_2 to the $X^+(^1D)$ atomic cation and an unusually short N−X bond.

The same bonding mechanism can be found in N_2H^+ ($N_2 \rightarrow H^+$) and also, as it is well established (see for instance ref 32 and references therein) in N_2O ($N_2 \rightarrow O(^1D)$).

AUTHOR INFORMATION

Corresponding Author

*E-mail: papakondylis@chem.uoa.gr. Telephone: +302107274565.

ORCID

Aristotle Papakondylis: 0000-0003-1534-2380

Notes

The author declares no competing financial interest.

REFERENCES

(1) Christe, K. O.; Wilson, W. W.; Sheehy, J. A.; Boatz, J. A. N_5^+: A Novel Homoleptic Polynitrogen Ion as a High Energy Density Material. *Angew. Chem., Int. Ed.* **1999**, *38*, 2004−2009.

(2) Moy, D.; Young, A. R., II The Preparation of Fluorodiazonium Hexafluoroarsenate from cis-Difluorodiazine. *J. Am. Chem. Soc.* **1965**, *87*, 1889−1892.

(3) Shamir, J.; Binenboym, J. The Laser Raman Spectrum of the N_2F^+ Cation. *J. Mol. Struct.* **1969**, *4*, 100−103.

(4) Christe, K. O.; Wilson, R. D.; Sawodny, W. The Vibrational Spectrum of the N_2F^+ Cation. *J. Mol. Struct.* **1971**, *8*, 245−253.

DOI: 10.1021/acs.jpca.6b10471
J. Phys. Chem. A 2016, 120, 9660−9666

(5) Pulay, P.; Ruoff, A.; Sawodny, W. Ab Initio Calculation of Force Constants for the Linear Molecules HCN, FCN, $(CN)_2$, and the Ion N_2F^+. *Mol. Phys.* **1975**, *30*, 1123−1131.
(6) Peters, N. J. S. Ab Initio Study of the Isoelectronic Series N_3^-, N_2O, and N_2F^+; Predicting the Bond Lengths in N_2F^+. *Chem. Phys. Lett.* **1987**, *142*, 76−78.
(7) Christe, K. O.; Wilson, R. D.; Wilson, W. W.; Bau, R.; Sukumar, S.; Dixon, D. A. The N_2F^+ Cation. An Unusual Ion Containing the Shortest Presently Known Nitrogen-Fluorine Bond. *J. Am. Chem. Soc.* **1991**, *113*, 3795−3800.
(8) Botschwina, P.; Sebald, P.; Bogey, M.; Demuynck, C.; Destombes, J. − L. The Millimeter-Wave Spectra of FN_2^+ and FCO^+ and Ab Initio Calculations for FCN, FN_2^+, FNC. *J. Mol. Spectrosc.* **1992**, *153*, 255−275.
(9) Cacace, F.; Grandinetti, F.; Pepi, F. Gaseous Fluorodiazonium Ions. Experimental and Theoretical Study on Formation and Structure of FN_2^+. *Inorg. Chem.* **1995**, *34*, 1325−1332.
(10) Bickelhaupt, F. M.; DeKock, R. L.; Baerends, E. J. The Short N−F Bond in N_2F^+ and how Pauli Repulsion Influences Bond Lengths. Theoretical Study of N_2X^+, NF_3X^+, and NH_3X^+ (X = F, H). *J. Am. Chem. Soc.* **2002**, *124*, 1500−1505.
(11) Harcourt, R. D. Valence Bond Studies of N_2F^+. *Aust. J. Chem.* **2003**, *56*, 1121−1125.
(12) Christe, K. O.; Dixon, D. A.; Grant, D. J.; Haiges, R.; Tham, F. S.; Vij, A.; Vij, V.; Wang, T.-H.; Wilson, W. W. Dinitrogen Difluoride Chemistry. Improved Syntheses of cis- and trans-N_2F_2, Synthesis and Characterization of $N_2F^+Sn_2F_9^-$, Ordered Crystal Structure of $N_2F^+Sb_2F_{11}^-$, High Level Electronic Structure Calculations of cis-N_2F_2, trans-N_2F_2, F_2N = N, and N_2F^+, and Mechanism of the trans-cis Isomerization of N_2F_2. *Inorg. Chem.* **2010**, *49*, 6823−6833.
(13) Dunning, T. H., Jr. Gaussian Basis Sets for Use in Correlated Molecular Calculations. I. The Atoms Boron through Neon and Hydrogen. *J. Chem. Phys.* **1989**, *90*, 1007−1023.
(14) Woon, D. E.; Dunning, T. H., Jr. Gaussian Basis Sets for Use in Correlated Molecular Calculations. III. The Atoms Aluminum through Argon. *J. Chem. Phys.* **1993**, *98*, 1358−1371.
(15) Wilson, A. K.; Woon, D. E.; Peterson, K. A.; Dunning, T. H., Jr. Gaussian Basis Sets for Use in Correlated Molecular Calculations. IV. The Atoms Galium through Krypton. *J. Chem. Phys.* **1999**, *110*, 7667−7675.
(16) Peterson, K. A.; Shepler, B. C.; Figgen, D.; Stoll, H. On the Spectroscopic and Thermochemical Properties of ClO, BrO, IO, and their Anions. *J. Phys. Chem. A* **2006**, *110*, 13877−13883.
(17) Raghavachari, K.; Trucks, G. W.; Pople, J. A.; Head-Gordon, M. A Fifth Order Perturbation Comparison of Electron Correlation Theories. *Chem. Phys. Lett.* **1989**, *157*, 479−483.
(18) Watts, J. D.; Gauss, J.; Bartlett, R. J. Coupled-Cluster Methods with Noniterative Triple Excitations for Restricted Open-Shell Hartree-Fock and other General Single Determinant Reference Functions. Energies and Analytical Gradients. *J. Chem. Phys.* **1993**, *98*, 8718−8733.
(19) Knowles, P. J.; Hampel, C.; Werner, H. − J. Coupled-Cluster Theory for High Spin Open Shell Reference Wave Functions. *J. Chem. Phys.* **1993**, *99*, 5219−5227.
(20) Werner, H.-J.; Knowles, P. J. An Efficient Internally Contracted Multiconfiguration−Reference Configuration Interaction Method. *J. Chem. Phys.* **1988**, *89*, 5803−5814.
(21) Davidson, E. R.; Silver, D. W. Size Consistency in the Dilute Helium Gas Electronic Structure. *Chem. Phys. Lett.* **1977**, *52*, 403−406.
(22) Werner, H.-J.; Knowles, P. J.; Knizia, G.; Manby, F. R.; Schütz, M. Molpro: A General-Purpose Quantum Chemistry Program Package. *WIREs Comput. Mol. Sci.* **2012**, *2*, 242−253.
(23) Werner, H.-J.; Knowles, P. J.; Lindh, R.; Manby, F. R.; Schütz, M.; Celani, P.; Korona, T.; Mitrushenkov, A.; Rauhut, G.; Shamasundar, K. R., et al. *MOLPRO 2012.1*; University College Cardiff Consultants Limited: 2012.
(24) Kramida, A.; Ralchenko, Yu.; Reader, J.; NIST ASD Team, NIST Atomic Spectra Database (ver. 5.1); National Institute of Standards and Technology: Gaithersburg, MD, http://physics.nist.gov/asd (retrieved September 15, 2016).
(25) Huber, K. P.; Herzberg, G. *Molecular Spectra and Molecular Structure IV. Constants of Diatomic Molecules*. Van Nostrand Reinhold Co: New York, 1979.
(26) Brites, V.; Hochlaf, M. Titan's Ionic Species. Theoretical Treatment of N_2H^+ and Related Ions. *J. Phys. Chem. A* **2009**, *113*, 11107−11111 and references therein..
(27) Amano, T.; Hirao, T.; Takano, J. Submillimeter-Wave Spectroscopy of HN_2^+ and DN_2^+ in the Excited Vibrational States. *J. Mol. Spectrosc.* **2005**, *234*, 170−175.
(28) Owrutsky, J. C.; Gudeman, C. S.; Martner, C. C.; Tack, L. M.; Rosenbaum, N. H.; Saykally, R. J. Determination of the Equilibrium Structure of Protonated Nitrogen by High Resolution Infrared Laser Spectroscopy. *J. Chem. Phys.* **1986**, *84*, 605−617.
(29) *CRC Handbook of Chemistry and Physics*, 84th ed.; Lide, D. R., Ed.; CRC Press: 2003; pp 9−20.
(30) Novak, I. Molecular and Electronic Structure of Bromoamines. *Heteroat. Chem.* **1994**, *5*, 145−148.
(31) Christe, K. O.; Dixon, D. A. A Quantitative Scale for the Oxidizing Strength of Oxidative Fluorinators. *J. Am. Chem. Soc.* **1992**, *114*, 2978−2985.
(32) Daud, M. N.; Balint-Kurti, G. G.; Brown, A. Ab Initio Potential Energy Surfaces, Total Absorption Cross Sections, and Product Quantum State Distributions for the Low-Lying Electronic States of N_2O. *J. Chem. Phys.* **2005**, *122*, 054305.

DOI: 10.1021/acs.jpca.6b10471
J. Phys. Chem. A 2016, 120, 9660−9666